EARTH SCIENCES

Recovery of an oxidized majorite inclusion from Earth's deep asthenosphere

Cheng Xu,[1]* Jindřich Kynický,[2,3] Renbiao Tao,[1,4] Xi Liu,[1] Lifei Zhang,[1]* Miroslav Pohanka,[2,3] Wenlei Song,[1,3] Yingwei Fei[1,4]*

Minerals recovered from the deep mantle provide a rare glimpse into deep Earth processes. We report the first discovery of ferric iron–rich majoritic garnet found as inclusions in a host garnet within an eclogite xenolith originating in the deep mantle. The composition of the host garnet indicates an ultrahigh-pressure metamorphic origin, probably at a depth of ~200 km. More importantly, the ferric iron–rich majoritic garnet inclusions show a much deeper origin, at least at a depth of 380 km. The majoritic nature of the inclusions is confirmed by mineral chemistry, x-ray diffraction, and Raman spectroscopy, and their depth of origin is constrained by a new experimental calibration. The unique relationship between the majoritic inclusions and their host garnet has important implications for mantle dynamics within the deep asthenosphere. The high ferric iron content of the inclusions provides insights into the oxidation state of the deep upper mantle.

INTRODUCTION

Mantle convection in Earth's asthenosphere drives plate tectonics (*1*). Tectonostratigraphic records and paleomagnetic data show that supercontinents have assembled and dispersed multiple times throughout geologic history. The assembly of the ancient supercontinent Columbia led to global-scale mountain building between 2.1 and 1.8 Ga (billion years ago) (*2*, *3*). Mantle upwelling and subduction-related processes provide scientists rare opportunities to access samples from the deep mantle. Preservation of high-pressure mantle minerals in ultrahigh-pressure rocks from that period of Earth's history can yield important information about the evolution and dynamics of the mantle. Here, we report the discovery of a high-pressure Fe^{3+}-rich majorite in an orogenic carbonatite from the Trans–North China Orogen (TNCO) formed at the end of oceanic subduction during the Paleoproterozoic era (~1.85 Ga) (*4*). This is the first conclusive finding of majorite in an eclogite xenolith, and its formation depth and mineral chemistry record an unusual mantle dynamic process in the asthenosphere.

RESULTS AND DISCUSSION

We found eclogite xenoliths (high-pressure metamorphic rocks of mafic composition) associated with carbonatite from the TNCO (fig. S1). The xenoliths are small (~70 mm in diameter) and extremely rare and are intruded by carbonatite veinlets. The matrix of the xenoliths contains garnet and omphacite. The garnet grains (up to ~7 mm in diameter) can be divided into two groups on the basis of their chemical composition (Table 1), which we designate as Grt-I and Grt-II. Both Grt-I and Grt-II contain omphacite, kyanite, quartz, apatite, and rutile inclusions. On the basis of its high Ca and low Cr contents, Grt-I is clearly eclogitic, formed from a basaltic protolith (*5*). In contrast, Grt-II grains have moderate Ca and high Cr, consistent with a websteritic protolith (intermediate between eclogite and peridotite). The Grt-II has a slight majorite component with an elevated Cr content and gives an equilibration pressure of 6.4 GPa (~200 km), using the empirical relationship between pressure and cation substitutions in the majoritic garnet (*6*).

The deep origin of the eclogite xenolith is consistent with reports indicating the possible subduction of continental materials to depths greater than 200 km in the region, which is based on mineral exsolutions in garnet within eclogites from Yangkou in the Chinese Sulu ultrahigh-pressure metamorphic belt (*7*). What is new in our eclogite xenoliths is the discovery of majoritic garnet inclusions in Grt-II. The granular majoritic inclusions have clearly defined grain boundaries and range from 100 to 300 μm in diameter (Fig. 1, A and B). In sharp contrast to Grt-I and Grt-II, the majorite grains contain no silicate inclusions, indicating a different origin. Table 1 provides the compositions of the majorite inclusions compared with those of Grt-I and Grt-II. The majorite inclusions show a clear excess of Si [3.15 to 3.22 per formula unit (pfu)] and concomitant Al deficit (~0.6 pfu) and contain relatively high MgO [~27.16 weight % (wt %)] and low CaO (~1.35 wt %) contents compared with the host garnet (Grt-II). In contrast to Grt-I and Grt-II, the majorite inclusions appear to be from a peridotitic protolith, on the basis of the low CaO and high Cr_2O_3 contents and the relationships among the divalent, trivalent, and quadrivalent cations (*5*, *8*).

To provide further evidence for the majoritic nature of the inclusions, we present Raman, Mössbauer, and x-ray diffraction (XRD) measurements. Figure 1C shows the Raman spectrum of the inclusion compared with that of garnet and synthetic majorite. The spectrum of the inclusion is distinct from that of Grt-I and the host Grt-II, which is identical to the garnet spectrum (Fig. 1C). On the basis of Raman spectra for compositions along the $Mg_3Al_2Si_3O_{12}$-$MgSiO_3$ binary, the inclusions have several features in the high-frequency region between 800 and 1100 cm^{-1} (centered at around the ν_1 stretching mode of the SiO_4 tetrahedra) that are consistent with a majorite component (*9*, *10*). The ν_1 stretching mode of the majorite inclusion is shifted to 925 cm^{-1} with new peaks at 1069 and 1089 cm^{-1} that are associated with the interaction of six-coordinated Si with oxygen and four-coordinated Si. We also observed the same set of peaks in the synthetic majorite but with broadening peak width in this frequency region (Fig. 1C). The Raman features in the intermediate- and low-frequency regions caused by the bending motions of the SiO_4 tetrahedra (ν_2 and ν_4) and the lattice vibrations, respectively, are more complicated, but the peak at 675 cm^{-1} is unique to majorite and is also observed in the synthetic majorite at 686 cm^{-1}. We observed more peaks in the intermediate- and low-frequency regions for the inclusion

[1]Key Laboratory of Orogenic Belt and Crustal Evolution, School of Earth and Space Sciences, Peking University, Beijing 100871, China. [2]Department of Geology and Pedology, Mendel University, 613 00 Brno, Czech Republic. [3]Central European Institute of Technology, Brno University of Technology, 616 00 Brno, Czech Republic. [4]Geophysical Laboratory, Carnegie Institution of Washington, Washington, DC 20015, USA.
*Corresponding author. Email: yfei@carnegiescience.edu (Y.F.); xucheng1999@pku.edu.cn (C.X.); lfzhang@pku.edu.cn (L.Z.)

Table 1. Compositions of garnets (Grt-I and Grt-II) and majorite. Compositions for synthetic majorites at 12.5 and 14 GPa are also listed for comparison.

	Natural samples			Synthetic majorite	
	Grt-I(6)*	Grt-II(4)	Majorite(6)	*P* = 12.5 GPa	*P* = 14 GPa
SiO_2	40.31(17)†	42.40(46)	44.20(38)	43.89(24)	44.03(16)
TiO_2	0.06(4)	0.10(2)	0.10(2)	0	0
Al_2O_3	22.54(21)	22.13(118)	7.09(41)	10.75(65)	10.80(93)
Cr_2O_3	0.04(4)	1.09(85)	1.10(44)	1.69(5)	1.61(9)
FeO‡	17.05(24)	7.71(9)	18.47(103)	15.94(75)	15.58(81)
MnO	0.71(11)	0.30(3)	0.32(5)	0	0
MgO	11.39(27)	20.79(35)	27.16(28)	25.10(22)	25.25(16)
CaO	8.01(27)	5.06(43)	1.35(32)	1.28(7)	1.31(4)
Na_2O	0.02(1)	0.02(1)	0.03(1)	0	0
Total	100.14(29)	99.60(20)	99.83(6)	98.71(33)	98.63(32)
Cations per 12 oxygen atoms§					
Si	3.003(11)	3.014(36)	3.181(28)	3.192(8)	3.199(19)
Ti	0.003(2)	0.006(1)	0.005(1)	0	0
Al	1.979(13)	1.854(97)	0.602(35)	0.921(52)	0.925(76)
Cr	0.002(2)	0.061(48)	0.063(25)	0.097(3)	0.092(5)
Fe^{3+}	0.005(15)	0.046(32)	0.963(69)	0.598(44)	0.585(46)
Fe^{2+}	1.057(5)	0.413(39)	0.148(54)	0.371(9)	0.362(17)
Mn	0.045(7)	0.018(2)	0.020(3)	0	0
Mg	1.265(27)	2.203(38)	2.914(26)	2.721(14)	2.735(12)
Ca	0.639(23)	0.385(31)	0.104(24)	0.100(5)	0.102(4)
Na	0.003(1)	0.002(1)	0.004(2)	0	0
$Fe^{3+}/\Sigma Fe$	0.02(2)	0.11(8)	0.87(5)	0.62(2)	0.62(2)
$X^{cat}Mj$¶		0.022(10)	0.193(29)	0.192(21)	0.199(32)
P(GPa)‖		6.4(0.4)	12.9(1.1)	12.9(0.8)	13.2(1.3)

*Number of electron microprobe analyses. †1 SD in the rightmost digit. ‡Total iron oxide. §Fe^{3+} and Fe^{2+} are calculated using the charge balance method. ¶$X^{cat}Mj = 0.5 \times (XMj1 + XMj2)$, where $XMj1 = (Si + Ti - 3) + Na$ and $XMj2 = 1 - 0.5 \times (Al + Cr + Fe^{3+}) + 1.25 \times Na$. ‖The pressures were calculated using our calibrated equation $P(GPa) = 5.61 + (37.98 \times X^{cat}Mj)$, with $Fe^{3+}/\Sigma Fe \sim 0.55$.

compared to those of the normal garnet. The observed spectral features in the intermediate- and low-frequency regions appear to be more consistent with those of the end-member $MgSiO_3$ majorite, which are due to the tetragonal distortion (*10*). The high ferric iron content in the majorite inclusion might be responsible for the local distortion caused by the substitution of Fe^{3+} in the structure. Further, the sharp Raman peaks of the majorite inclusion are consistent with local ordering due to extensive low-temperature annealing. Further investigation of the crystal chemistry of the majorite inclusion is required to understand the spectral features, especially in the low-frequency region.

The inclusions were large enough (100 to 300 μm) for us to separate them from the host without any contamination and perform both Mössbauer spectroscopic and XRD measurements. Figure 2A shows the Mössbauer spectrum of the separated inclusions. The quadrupole splitting and isomer shift of Fe^{3+} and Fe^{2+} are consistent with the hyperfine parameters and site occupancies in the majorite structure (*11*). One of the distinctive chemical features of the majorite inclusions is the very high ferric iron content ($Fe^{3+}/\Sigma Fe = 0.81 \pm 0.01$), which is determined by area ratios of Fe^{3+} in the octahedral site and Fe^{2+} in the dodecahedral site (Fig. 2A). Calculations by charge balance also yielded similar high Fe^{3+} content ($Fe^{3+}/\Sigma Fe = 0.87 \pm 0.05$) (Table 1). The measured Fe^{3+} content is exceptionally high for what is expected for a majorite in peridotitic mantle and is comparable to majorite synthesized under highly oxidized conditions (*11*, *12*).

We used the same separated inclusions for XRD measurements. The XRD data of the separated inclusions can be indexed with a cubic

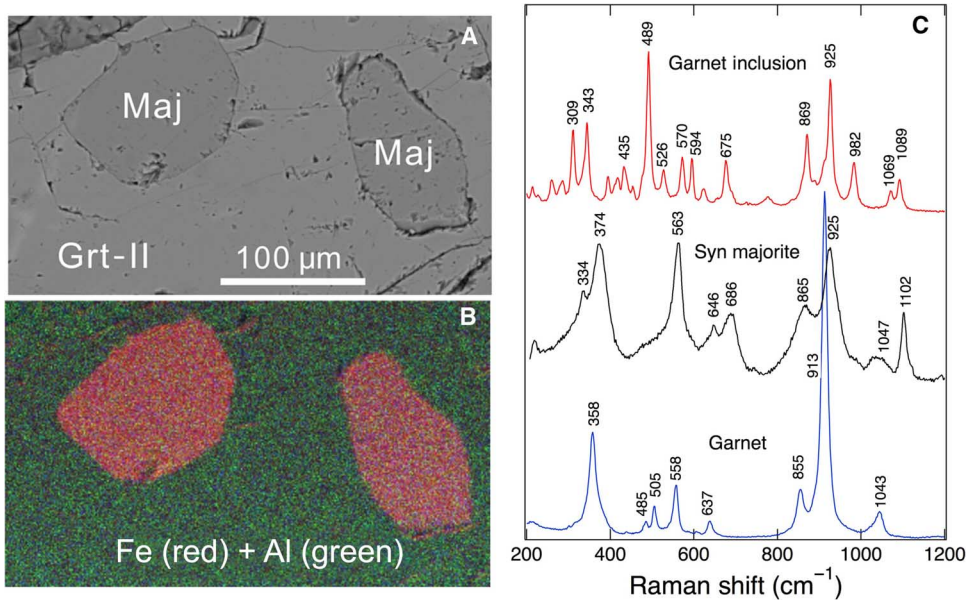

Fig. 1. Majoritic inclusions in garnet with Raman spectra. (**A**) Backscattered electron (BSE) image of majorite inclusion (Maj) in the host garnet (Grt-II). (**B**) Superposed Fe and Al x-ray mapping shows higher Fe and lower Al contents in majorite inclusion than those in the host garnet. (**C**) The Raman spectrum of the inclusion in garnet compared with that of the synthetic majorite and garnet (Grt-I or Grt-II).

unit cell parameter, a = 11.5675(2) Å (Fig. 2B and Table 2), clearly showing a garnet group mineral. The structure of the majoritic garnet with a low fraction of majoritic component (<0.3) is expected to be cubic (*13*). The combination of the cubic structure and excess of Si provides a definitive identification of the inclusion as a majoritic garnet. The cubic structure of the inclusion is also crucial for ruling out other possible decomposition products, such as pyroxene, because mantle majorite always decomposes into a low-pressure phase assemblage (pyroxene + garnet) upon exhumation. We observed no diffraction peaks of pyroxene in the XRD data of the separated inclusions. In comparison, the host garnet (Grt-II) has a slightly smaller unit cell parameter, a = 11.5634(6) Å, and almost no ferric iron (Table 1). The smaller unit cell parameter is consistent with the lower iron content in the host garnet.

We have now established that the inclusions are the Fe^{3+}-rich majoritic garnet by mineral chemistry, Raman spectroscopy, XRD, and Mössbauer measurements. The majorite substitution into garnet occurs only at high pressure, and the composition of the majoritic garnet is an excellent indicator of the depth of origin when it occurs in ultrahigh-pressure rocks (*14*–*17*) or diamonds (*18*–*20*). However, our majorite inclusions have an extremely high Fe^{3+} content, and there is no barometer that takes account of the ferric iron component in majorite. Applying the available experimental data summarized in the study by Collerson *et al.* (*6*), the Si^{4+} excess in the majorite inclusions indicates a formation pressure between 10 and 14 GPa, whereas the Al^{3+} deficit would place the pressure above 17 GPa, assuming all iron in Fe^{2+}. If one includes Fe^{3+} with Cr^{3+} and Al^{3+} in the barometer proposed by Collerson *et al.* (*6*), the pressure reduces to 9.3 GPa. The large uncertainty in the pressure calculation reflects a lack of knowledge about the role of ferric iron in the calibration. To further constrain the formation pressure, we have performed a series of experiments in the pressure range of 6.5 to 15 GPa, using a starting composition similar to that of the majorite inclusions (see Materials and Methods). The experiments produced synthetic majorites with high Fe^{3+} ($Fe^{3+}/\Sigma Fe$ ~ 0.5 to 0.6) and low Al^{3+} contents (table S1). Table 1 lists the compositions of two run products recovered from 12.5 and 14 GPa compared with those of the majorite inclusions. Figure 3 plots the relationship between pressure and X^{cat}Mj, as defined by Collerson *et al.* (*6*). Here, we include Fe^{3+} with Cr^{3+} and Al^{3+} (see footnote "¶" in Table 1). The experimental results define a linear trend, where P(GPa) = 5.61 (± 0.40) + 37.98 (± 2.29) × X^{cat}Mj. The linear relationship for $Fe^{3+}/\Sigma Fe$ ~ 0.55 has a significantly higher slope compared to the barometer proposed by Collerson *et al.* (*6*) for $Fe^{3+}/\Sigma Fe$ = 0. Using our new calibration, we obtain a pressure of 12.9 ± 1.1 GPa (corresponding to a depth of ~380 km) for the majorite inclusions (Fig. 3). This is a lower bound because the majorite inclusion has a higher $Fe^{3+}/\Sigma Fe$ ratio (~0.8) than majorites in our experiments and pressure is positively correlated to the $Fe^{3+}/\Sigma Fe$ ratio.

The synthetic majorites (at 12.5 and 14 GPa) and the natural majorite have very similar chemical compositions, except for the fact that the Fe^{3+} and Al^{3+} contents are reversed. The Si^{4+} excess in the synthetic majorite is comparable to that in the natural majorite inclusions (Table 1). We also compared the XRD data of the synthetic and natural majorites. The observed diffraction peaks are identical to each other, with comparable unit cell parameters (Table 2).

The new experimental results further strengthen our claim of the majorite identity of the inclusion and show that the majorite inclusion records depths greater than 380 km. The central question is how a majorite that originated near the 410-km discontinuity could be trapped in a garnet formed at a much shallower depth, perhaps at ~200 km. The compositional difference and textural relations between the majorite inclusions and their host garnet certainly do not support a common origin. The apparent different formation depths rule out the possibility that the majorite inclusions represent exsolved phases due to a very high Fe^{3+} content in the garnet. The likely explanation is that the majoritic inclusion formed deep but was transported to the shallower mantle, where it was captured and encapsulated by a garnet overgrowth (for example, Grt-II). This model requires an unusual dynamic process to quickly transport the majorite from a depth of ~400 to 200 km without decomposing the majorite.

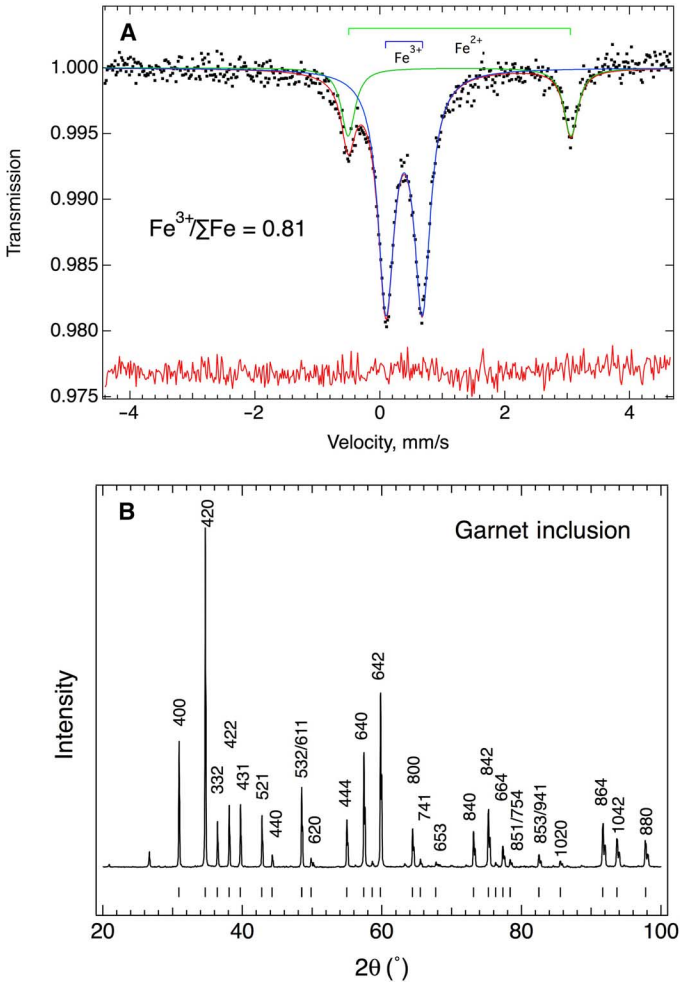

Fig. 2. Mössbauer spectrum and XRD pattern of the separated majorite inclusions. (**A**) The fitted Mössbauer spectrum, yielding quadrupole splittings and isomer shifts of 3.567(9) and 1.275(5) mm/s for Fe^{2+}, respectively, and 0.580(3) and 0.388(2) mm/s for Fe^{3+}, respectively. The area fraction $Fe^{3+}/\Sigma Fe$ is 0.81(1). (**B**) XRD pattern of the separated inclusions, labeled with Miller indices (*hkl*). The vertical ticks at the bottom of the diffraction pattern indicate the calculated peaks with a cubic unit cell parameter, a = 11.5675 Å.

Table 2. The indexed peaks of the XRD pattern of the majorite (Mj) inclusion and synthetic majorite recovered from 14 GPa. The calculated d spacings (d_{calc}) with a cubic unit cell parameter, a = 11.5675(2) Å, agree well with the observed d spacings (d_{obs}) for the natural majorite inclusion. The synthetic majorite has a comparable unit cell parameter, a = 11.5688(54) Å.

			Natural Mj			Synthetic Mj
h	*k*	*l*	d_{obs} (Å)	d_{calc} (Å)	$d_{obs} - d_{calc}$ (Å)	d_{obs} (Å)
4	0	0	2.8921	2.8919	0.0002	2.8957
4	2	0	2.5862	2.5866	−0.0004	2.5912
3	3	2	2.4667	2.4662	0.0005	2.4627
4	2	2	2.3613	2.3612	0.0001	2.3615
4	3	1	2.2686	2.2686	0.0000	2.2742
5	2	1	2.1122	2.1119	0.0003	2.1116
4	4	0	2.0448	2.0449	−0.0001	—
5	3	2	1.8767	1.8765	0.0002	1.8759
6	2	0	1.8290	1.8290	0.0000	1.8324
4	4	4	1.6697	1.6696	0.0001	1.6704
6	4	0	1.6041	1.6041	0.0000	1.6033
6	4	2	1.5457	1.5458	−0.0001	1.5456
8	0	0	1.4459	1.4459	0.0000	1.4465
7	4	1	1.4242	1.4239	0.0003	1.4223
6	5	3	1.3823	1.3826	−0.0003	1.3821
8	4	0	1.2933	1.2933	0.0000	1.2928
8	4	2	1.2620	1.2621	−0.0001	1.2624
7	6	1	1.2474	1.2474	0.0000	1.2471
6	6	4	1.2332	1.2331	0.0001	1.2337
8	5	1	1.2193	1.2193	0.0000	1.2188
8	5	3	1.1685	1.1685	0.0000	1.1674
10	2	0	1.1343	1.1343	0.0000	1.1345
8	6	4	1.0739	1.0740	−0.0001	1.0734
10	4	2	1.0561	1.0560	0.0001	1.0556
8	8	0	1.0224	1.0224	0.0000	1.0226

Here, we suggest two possible mechanisms to transport the majoritic inclusions from ~400 to 200 km: (i) transport in a carbonate-bearing melt or (ii) transport during a high-temperature mantle upwelling. It is possible that the majorite was quickly transported by low-viscosity, fast-rising carbonatitic magma (*21*). Carbonate-bearing oceanic crust can melt at depths of approximately 300 to 700 km because of a deep depression along the melting curve over this depth range (*22*, *23*). Carbonatitic magmas with an origin in the mantle transition zone have also been previously inferred from mineral inclusions in diamonds (*24*). In this scenario, the involvement of carbonatitic magma may also provide a viable mechanism to form high Fe^{3+}-bearing majorite through redox reactions. The high $Fe^{3+}/\Sigma Fe$ ratio in the majoritic garnet can be produced through the reduction of carbonate accompanied by oxidizing the iron component in the reducing mantle (*25*). The residual carbonatitic magmas could facilitate the rapid ascent of mantle materials.

The second possibility is that mantle upwelling before the Paleoproterozoic was responsible for bringing the majorite to shallow depths, similar to the multigenerational formation of the ultradeep mantle rocks of western Norway (*26*). This would explain the peridotitic origin of the majorite inclusions and imply that the deep upper mantle and possibly the transition zone are intrinsically enriched in ferric iron and hence a highly oxidized environment. The process may involve high-temperature decompression melting. It would be difficult to reconcile with the preservation of majorite unless the involvement of volatiles can substantially decrease the melting temperature. The implication for a highly oxidized mantle is also at odds with the conventional wisdom of the redox state of the mantle supporting a more reduced mantle (*25*, *27*). This mechanism of recovery for the majorite inclusions can only be possible if the Fe^{3+}-rich majorite is exceptionally stable

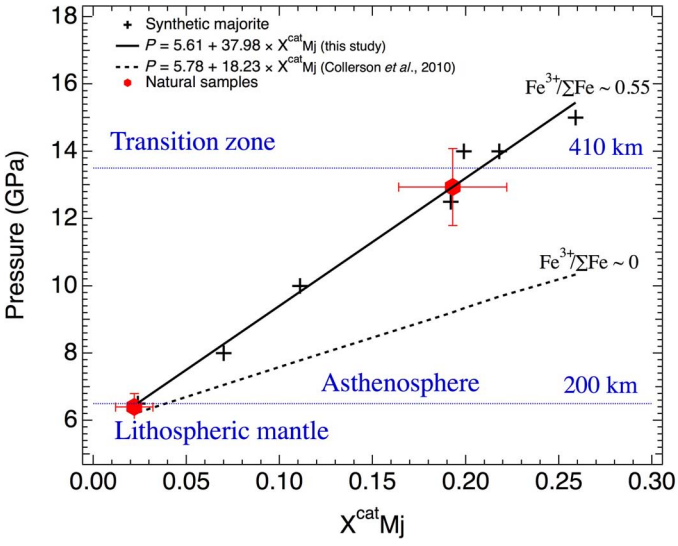

Fig. 3. Estimated pressures for the formation of the majoritic garnets. The relationship between pressure and composition parameter X^{cat}Mj defined by Collerson *et al.* (*6*) is experimentally determined for Fe^{3+}-bearing majorite. The crosses represent the experimental data of the synthetic majorites (table S1). The solid line represents the best fit to the data with an average $Fe^{3+}/\Sigma Fe$ of 0.55. The calculated pressures for the natural samples are indicated by solid hexagons. The relationship between pressure and cation substitutions in the majoritic garnet without considering the effect of ferric iron (*6*) is also shown for comparison (dashed line).

and has a high kinetic barrier for the back-transformation at low pressure; otherwise, we would expect the back-transformation of majorite to garnet plus clinopyroxene upon exhumation, as is commonly seen in majoritic inclusions in diamond.

Regardless of the actual transport mechanism, it is certain that the high-pressure mineral must rapidly ascend to a relatively cold environment to preserve the structure and composition of the majorite. The eclogite xenolith hosting the majorite inclusions was exhumed within an ancient subduction environment; thus, it is likely that the Fe^{3+}-rich majorite was captured in a cold subduction environment that allowed for the preservation of the inclusion while the host garnet grew around it. The cold subduction environment is supported by the estimated equilibrium temperatures of the host garnets in the range of 670° to 1000°C for depths of 100 to 200 km, using the garnet-clinopyroxene Fe-Mg geothermometer (*28*).

We favor a two-stage transport model, where the Fe^{3+}-rich majorite was first rapidly transported from ~400 km to a relatively cold subduction environment at the bottom of the lithospheric mantle (~200 km) and then encapsulated by a garnet overgrowth. The majorite inclusions and their host were then brought to the surface as a xenolith in subduction-related carbonatitic magma. The carbonatite associated with the eclogite xenolith has signatures of the subducted oceanic crust and clearly played a critical role in transporting the eclogite xenolith to the surface. We speculate that carbonatitic magma, which is different from shallow magma, might have been involved in producing Fe^{3+}-rich majorite at the bottom of the asthenosphere, and the nature of that deep carbonatitic magma is less clear.

We have discovered the first sample of the Fe^{3+}-rich majorite in a host garnet and established a new barometer for Fe^{3+}-bearing majorites to precisely determine the formation depth of the Fe^{3+}-rich majorite. The composition of the natural majorite is consistent with an origin of deep upper mantle (~380 km depth). The high Fe^{3+} content in the majorite inclusions might be a product of a redox reaction involving carbonatitic magmas. It has likely played an important role in the preservation because the Fe^{3+}-rich majorite is kinetically more stable than normal mantle majorite. The host garnet and majorite inclusion record two distinctive depths in the asthenosphere, which has important implications for the evolution and convection of the mantle during ancient supercontinent assembly and breakup. The preservation of the Fe^{3+}-rich majorite, particularly in a host garnet, provides a rare opportunity to understand the mantle chemistry and dynamic process.

MATERIALS AND METHODS

Chemical analysis

The chemical compositions of the minerals were obtained by wavelength-dispersive x-ray spectrometry using a Cameca SX100 electron microprobe at the Masaryk University, Czech Republic. The microprobe was operated at an accelerating voltage of 15 kV and a beam current of 20 nA. A TESCAN Integrated Mineral Analyzer, equipped with a first-class ultrafast scintillator BSE detector, four silicon drift energy-dispersive x-ray (EDX) detectors, and a secondary electron detector, was used to acquire the BSE and EDX data to generate the element mapping and BSE images. The samples were analyzed in high-vacuum mode with an accelerating voltage of 25 kV and a probe current of 5 nA. The chemical compositions of the synthetic majorites were determined with a field-emission electron microprobe (JEOL JXA-8530F) at the Geophysical Laboratory, Carnegie Institution of Washington. The sample was analyzed with an accelerating voltage of 15 kV and a probe current of 30 nA.

XRD analysis

The majorite inclusions were separated from the host garnet (Grt-II) using a thin diamond cutter. The separated inclusions were hand-picked and checked under a Leica stereomicroscope and a Keyence three-dimensional microscope. The crystal grain was x-rayed with an X'Pert Pro MPD system, which included a glass collimating monocapillary to reduce the x-ray beam size to ~100 μm and a multichannel position-sensitive detector (automatically correcting the sample-detector distance) at the XRD Laboratory, Institute of Criminalistics Prague (www.xray.cz/xray/csca/kol2006/abst/kotrly.htm). The x-ray data from 5° to 100° 2θ were collected with a scanning step of 0.017° 2θ. The instrument used a Cu target (1.540562 Å) and was operated at a voltage of 40 kV and an electrical current of 40 mA. A detailed description of the x-ray microdiffractometer can be found in the study by Kotrlý (*29*). The recovered synthetic samples were loaded on a flat sample holder to collect multicrystal XRD patterns with a Bruker D8 Discover diffractometer at the Geophysical Laboratory. The instrument was operated at 50 kV and 1000 mA with an area detector and Mo Kα radiation.

Raman spectroscopic measurements

Raman spectra of the natural and synthetic samples were collected using a LabRAM HR Evolution (HORIBA Jobin Yvon) spectrometer system at the Masaryk University and a JASCO NRS-3100 confocal micro-Raman spectrometer at the Geophysical Laboratory, respectively. The spectra of the natural samples were recorded with a polarized light, using an output power of 34 mW of frequency-doubled Nd:YAG laser (at 532 nm). The wave-number calibration was carried out using the Rayleigh line and Ne lamp emissions. The spectra of the synthetic

samples were also collected with a laser excitation wavelength of 532 nm.

Mössbauer spectroscopy

Transmission ^{57}Fe Mössbauer spectra were collected at the Regional Centre of Advanced Technologies and Materials, Palacký University, Czech Republic. The spectra were accumulated at room temperature in constant acceleration mode using a ^{57}Co(Rh) source (1.85 gigabecquerel). We handpicked the majorite inclusions and prepared the separated grains in the form of a conventional absorber (Fe, ~5 mg cm^{-2}). The data were collected at room temperature. The isomer shift (δ) was calibrated against an α-Fe foil at room temperature. Spectra were folded and fitted by Lorentzian functions using the program CONFIT2000.

Synthesis experiments

The majorite synthesis experiments were carried out in a multi-anvil device at the Geophysical Laboratory. A sintered oxide mix with a composition similar to that of the natural majorite was used as the starting material for the high-pressure experiments. Ferric iron was introduced as Fe_2O_3 in the mix. The starting material was loaded into a Pt capsule and ran in a 14/8 (14-mm octahedron edge length/8-mm truncation edge length of a tungsten carbide cube) cell assembly using a 1500-ton multi-anvil press. Pressure was calibrated using fixed-phase transition points, and temperature was measured with a type C thermocouple. Table S1 provides the chemical compositions of the synthetic majorite in equilibrium with pyroxene and olivine (fig. S2) at pressures from 6.5 to 15 GPa.

SUPPLEMENTARY MATERIALS

Supplementary material for this article is available at http://advances.sciencemag.org/cgi/content/full/3/4/e1601589/DC1

table S1. Compositions of synthetic majorites.

fig. S1. Field observations of eclogite xenoliths associated with carbonatite in the North China Craton.

fig. S2. BSE image of a representative run product at 12.5 GPa and 1600°C, showing the majoritic garnet (Maj) in equilibrium with pyroxene (Px) and olivine (Ol).

REFERENCES AND NOTES

1. D. Breuer, T. Spohn, Possible flush instability in the mantle convection at the Archean–Proterozoic transition. *Nature* **378**, 608–610 (1995).
2. J. J. W. Rogers, M. Santosh, Configuration of Columbia, a Mesoproterozoic supercontinent. *Gondwana Res.* **5**, 5–22 (2002).
3. G. Zhao, M. Sun, S. A. Wilde, S. Li, A Paleo-Mesoproterozoic supercontinent: Assembly, growth and breakup. *Earth Sci. Rev.* **67**, 91–123 (2004).
4. G. Zhao, M. Sun, S. A. Wilde, S. Li, Late Archean to Paleoproterozoic evolution of the North China Craton: Key issues revisited. *Precambrian Res.* **136**, 177–202 (2005).
5. E. S. Kiseeva, G. M. Yaxley, A. S. Stepanov, H. Tkalčić, K. D. Litasov, V. S. Kamenetsky, Metapyroxenite in the mantle transition zone revealed from majorite inclusions in diamonds. *Geology* **41**, 883–886 (2013).
6. K. D. Collerson, Q. Williams, B. S. Kamber, S. Omori, H. Arai, E. Ohtani, Majoritic garnet: A new approach to pressure estimation of shock events in meteorites and the encapsulation of sub-lithospheric inclusions in diamond. *Geochim. Cosmochim. Acta* **74**, 5939–5959 (2010).
7. K. Ye, B. L. Cong, D. N. Ye, The possible subduction of continental material to depths greater than 200 km. *Nature* **407**, 734–736 (2000).
8. E. S. Kiseeva, B. J. Wood, S. Ghosh, T. Stachel, The pyroxenite-diamond connection. *Geochem. Perspect. Lett.* **2**, 1–9 (2016).
9. A. M. Hofmeister, P. A. Giesting, B. Wopenka, G. D. Gwanmesia, B. L. Jolliff, Vibrational spectroscopy of pyrope-majorite garnets: Structural implications. *Am. Mineral.* **89**, 132–146 (2004).
10. P. F. McMillan, R. J. Hemley, P. Gillet, Vibrational spectroscopy of mantle minerals, in *Mineral Spectroscopy: A Tribute to Roger G. Burns*, M. D. Dyar, C. McCammon, M. W. Schaefer, Eds. (Geochemical Society, 1996), pp. 175–213.
11. C. A. McCammon, N. L. Ross, Crystal chemistry of ferric iron in (Mg,Fe)(Si,Al)O_3 majorite with implications for the transition zone. *Phys. Chem. Miner.* **30**, 206–216 (2003).
12. A. Rohrbach, C. Ballhaus, U. Golla–Schindler, P. Ulmer, V. S. Kamenetsky, D. V. Kuzmin, Metal saturation in the upper mantle. *Nature* **449**, 456–458 (2007).
13. A. Nakatsuka, A. Yoshiasa, T. Yamanaka, O. Ohtaka, T. Katsura, E. Ito, Symmetry change of majorite solid-solution in the system $Mg_3Al_2Si_3O_{12}$-$MgSiO_3$. *Am. Mineral.* **84**, 1135–1143 (1999).
14. K. D. Collerson, S. Hapugoda, B. S. Kamber, Q. Williams, Rocks from the mantle transition zone: Majorite-bearing xenoliths from Malaita, southwest Pacific. *Science* **288**, 1215–1223 (2000).
15. S. E. Haggerty, V. Sautter, Ultradeep (greater than 300 kilometers), ultramafic mantle xenoliths. *Science* **248**, 993–996 (1990).
16. V. Sautter, S. E. Haggerty, S. Field, Ultradeep (>300 km) ultramafic xenoliths: Petrological evidence from the transition zone. *Science* **252**, 827–830 (1991).
17. H. L. M. van Roermund, M. R. Drury, Ultra-high pressure (P > 6 GPa) garnet peridotites in Western Norway: Exhumation of mantle rocks from >185 km depth. *Terra Nova* **10**, 295–301 (1998).
18. T. Stachel, Diamonds from the asthenosphere and the transition zone. *Eur. J. Mineral.* **13**, 883–892 (2001).
19. R. Tappert, T. Stachel, J. W. Harris, K. Muehlenbachs, T. Ludwig, G. P. Brey, Subducting oceanic crust: The source of deep diamonds. *Geology* **33**, 565–568 (2005).
20. B. Harte, Diamond formation in the deep mantle: The record of mineral inclusions and their distribution in relation to mantle dehydration zones. *Mineral. Mag.* **74**, 189–215 (2010).
21. M. J. Genge, G. D. Price, A. P. Jones, Molecular dynamics simulations of $CaCO_3$ melts to mantle pressures and temperatures: Implications for carbonatite magmas. *Earth Planet. Sci. Lett.* **131**, 225–238 (1995).
22. K. D. Collerson, Q. Williams, A. E. Ewart, D. T. Murphy, Origin of HIMU and EM-1 domains sampled by ocean island basalts, kimberlites and carbonatites: The role of CO_2-fluxed lower mantle melting in thermochemical upwellings. *Phys. Earth Planet. Inter.* **181**, 112–131 (2010).
23. A. R. Thomson, M. J. Walter, S. C. Kohn, R. A. Brooker, Slab melting as a barrier to deep carbon subduction. *Nature* **529**, 76–79 (2016).
24. M. J. Walter, G. P. Bulanova, L. S. Armstrong, S. Keshav, J. D. Blundy, G. Gudfinnsson, O. T. Lord, A. R. Lennie, S. M. Clark, C. B. Smith, L. Gobbo, Primary carbonatite melt from deeply subducted oceanic crust. *Nature* **454**, 622–625 (2008).
25. C. A. McCammon, The paradox of mantle redox. *Science* **308**, 807–808 (2005).
26. M. Scambelluri, T. Pettke, H. L. M. van Roermund, Majoritic garnets monitor deep subduction fluid flow and mantle dynamics. *Geology* **36**, 59–62 (2008).
27. D. Frost, C. A. McCammon, The redox state of Earth's mantle.*Annu. Rev. Earth Planet. Sci.* **36**, 389–420 (2008).
28. E. J. Krogh, The garnet-clinopyroxene Fe-Mg-geothermometer—A reinterpretation of existing experimental data. *Contrib. Mineral. Petrol.* **99**, 44–48 (1988).
29. M. Kotrlý, Using X-ray diffraction in forensic science. *Z. Kristallogr.* **222**, 193–198 (2007).

Acknowledgments: We thank R. Škoda and M. Kotrlý for analysis assistance and H. O'Neill, K. Collerson, N. Bennett, and C. Jackson for providing comments on the manuscript. We also thank M. Walter and an anonymous reviewer for their constructive reviews of the manuscript. **Funding:** This research was financially supported by the Chinese "973" project (2013CB429800), the National Natural Science Foundation of China (41173033, 41520104004, and 41573033), and Czechic CEITEC 2020 (LQ1601). The high-pressure experiments were supported by the Carnegie Institution of Washington and an NSF Geochemistry grant EAR-1447311 (to Y.F.). **Author contributions:** C.X., J.K., Y.F., L.Z., and X.L. formulated the project. C.X., J.K., and W.S. were responsible for sample collections. C.X., J.K., M.P., Y.F., L.Z., and X.L. were responsible for mineralogy and petrology. Y.F. and R.T. performed high-pressure experiments. C.X. and Y.F. wrote the manuscript with inputs from the coauthors. **Competing interests:** The authors declare that they have no competing interests. **Data and materials availability:** All data needed to evaluate the conclusions in the paper are present in the paper and/or the Supplementary Materials. Additional data related to this paper may be requested from the authors.

Submitted 11 July 2016
Accepted 11 February 2017
Published 7 April 2017
10.1126/sciadv.1601589

Citation: C. Xu, J. Kynický, R. Tao, X. Liu, L. Zhang, M. Pohanka, W. Song, Y. Fei, Recovery of an oxidized majorite inclusion from Earth's deep asthenosphere. *Sci. Adv.* **3**, e1601589 (2017).

Science Advances

Recovery of an oxidized majorite inclusion from Earth's deep asthenosphere

Cheng Xu, Jindrich Kynický, Renbiao Tao, Xi Liu, Lifei Zhang, Miroslav Pohanka, Wenlei Song and Yingwei Fei

Sci Adv **3** (4), e1601589.
DOI: 10.1126/sciadv.1601589